LIMNOLOGY
and
OCEANOGRAPHY

ASLO

Limnol. Oceanogr. 00, 2017, n/a–n/a

doi: 10.1002/lno.10572

Elevated alkaline phosphatase activity in a phosphate-replete environment: Influence of sinking particles

Clare E. Davis ,* **Claire Mahaffey**
Department of Earth, Ocean and Ecological Sciences, University of Liverpool, Liverpool, UK

Abstract

Alkaline phosphatase activity (APA) is traditionally a proxy for phosphate (DIP)-limitation because it is induced by DIP-limited microbes to access the labile ester fraction of the organic phosphorus (OP) pool. Here, we present multi-year summertime depth distributions of APA and enzyme kinetics in the DIP-replete Celtic Sea. Our findings support the cumulating body of evidence that APA has a potentially widespread role in OP remineralization through the water column. APA and V_{max} were positively correlated with depth and DIP, with total APA being threefold higher below (0.93 ± 0.32 nM P h^{-1}) compared to above the thermocline (0.30 ± 0.24 nM P h^{-1}, $p < 0.001$). Separation of particles by sinking speed demonstrated that APA was eightfold higher on fast sinking (F_{fast}) particles compared to slow sinking particles (F_{slow}; $p < 0.05$). When normalized to particulate organic carbon (POC) and bacterial production (BP), APA_{POC} and APA_{BP} associated with F_{fast} (0.76 ± 0.10 nmol P μmol C^{-1} h^{-1}, 21.13 ± 2.2 nmol P nmol C^{-1}, respectively) were fourfold and 25-fold higher compared to the combined APA associated with dissolved plus suspended (F_{susp}) and F_{slow} fractions (0.19 ± 0.06 nmol P μmol C^{-1} h^{-1} and 0.84 ± 0.23 nmol P nmol C^{-1}, respectively). We postulate that this may reflect enhanced ectoenzyme activity associated with bacteria colonizing particle surfaces and/or release by zooplankton via faecal pellet excretion. Knowledge of the disparity between APA and BP associated with particle and dissolved phases is required to accurately define the O_2 : P ratio of regenerated P derived from sinking particles as a result of AP-facilitated remineralization.

Phosphorus (P) is an essential macronutrient for all life on Earth due to its role in key cellular components such as genetic biomolecules (DNA and RNA), energy transfer molecules (ATP) and cell structure (phospholipids; Karl and Björkman 2002). P availability may limit ocean productivity on geological timescales (Tyrrell 1999). Thus, understanding the P cycle is essential for coupling marine primary productivity and the global carbon (C) cycle.

Phytoplankton and bacterioplankton utilize dissolved inorganic phosphate (DIP) as a P source to support growth in preference to dissolved organic phosphorus (DOP; Björkman and Karl 1994). DOP is an array of organic molecules that range in size and complexity from relatively labile compounds like phosphomonesters to more refractory molecules like phosphonates (Kolowith et al. 2001). In the surface subtropical open ocean, DOP production is often decoupled from consumption. In combination with a long-lived refractory DOP pool ($\sim$ 40 nM; Karl and Björkman 2002), this decoupling results in DOP concentrations that can be 5–10 times higher than those of DIP (Mather et al. 2008; Reynolds et al. 2014), which may be chronically low ($<$ 10 nM, Mahaffey et al. 2014).

While DIP can be assimilated directly via a high affinity uptake pathway, DOP assimilation requires that the molecule first be remineralized to separate DIP from the C moiety. This is achieved using hydrolytic enzymes. Many marine microbes have the capacity to synthesize hydrolytic enzymes, like alkaline phosphatase (AP), to facilitate the remineralization of organic phosphorus (OP) to DIP. AP refers to a broad group of nonspecific phosphomonoesterases. Alkaline phosphatase activity (APA) can be induced by DIP-limited microbial communities when DIP concentrations are low and repressed under high DIP concentrations. As such, enhanced APA has commonly been used as an indicator of DIP-limitation in oligotrophic surface ocean regions (Lomas et al. 2010; Suzumura et al. 2012; Mahaffey et al. 2014).

In recent years, there has been an increase in the reporting of elevated APA under DIP-replete conditions and at depth (Hoppe and Ullrich 1999; Sebastián et al. 2004; Baltar et al. 2010; Duhamel et al. 2011; Labry et al. 2016). A

*Correspondence: davis@liverpool.ac.uk

Table 1. A summary of previously published AP enzyme kinetics data.*

Reference	Region	DIP (nM)	APA (nmol P L^{-1} h^{-1}) †(nmol P μg Chl a^{-1} L^{-1} h^{-1}) ‡(nmol P μg C^{-1} L^{-1} h^{-1})	V_{max} (nmol P h^{-1}) †(nmol P μg Chl a^{-1} h^{-1})	K_m (μM)
Duhamel et al. (2010)	NPSG	13–59	0.36–1.28	–	–
Duhamel et al. (2011)	NPSG	12–153	–	0.01–3.12	0.01–0.56
Sohm et al. (2008)	NPSG	0.036	†0.7–7.2	†0.2–2.8	0.05–2.8
Dyhrman and Ruttenberg (2006)	NEPC	2–85	0.94–3.18	–	–
Nicholson et al. (2006)	NEPC	<2400	<30,000	–	–
Suzumura et al. (2012)	NWP	11–26	–	0.26–1.59	0.13–1.36
Duhamel et al. (2011)	SPSG	–	–	0.03–0.61	0.26–1.26
Sohm et al. (2008)	NA	0.045	†0.05–0.1	†2.6–13.8	−0.16–0.38
Mather et al. (2008)	NA	–	‡0.84–4.65	–	789
Davis et al. (2014)	NEAC	–	0.2–1.3	–	–
Mather et al. (2008)	SA	–	‡0.2–0.84	–	565
Vidal et al. (2003)	CA	–	0–30	–	–
Sebastián et al. (2004)	EA	3–200	0.08–0.36	0.25–2.1	0.03–0.31
Sohm and Capone (2006)	SS	–	†3.1–83.9	–	–
Lomas et al. (2010)	SS	–	7.9–12.5	–	–
Orchard et al. (2010)	SS	0.5–10.6	†0–42	†54	0.29
Li et al. (1998)	GoA	–	40–150	–	–
Sohm et al. (2008)	NAus	0.11	†0.08	†0.2–4	0.05–0.33
This study	NEAC	60–760	0.04–1.54 †0.14–23.6 ‡0.0003–0.30	0.09–1.91 †0.09–46.9	34.2–3143

* Note: Details provided of studies include location, range in phosphate concentration (DIP, nM), volumetric and biomass normalized rates of APA, and enzyme kinetic parameters V_{max} and K_m (μM). † and ‡ denote change of units between volumetric and biomass normalized rates. Regions are North Pacific Subtropical Gyre (NPSG), North East Pacific Coast (NEPC), North West Pacific (NWP), South Pacific Subtropical Gyre (SPSG), North Atlantic (NA), North East Atlantic Coast (NEAC), South Atlantic (SA), Central Atlantic (CA), Equatorial Atlantic (EA) and Sargasso Sea (SS), Gulf of Aqaba (GoA), and North Australia (NAus).

number of explanations have been given for these observations. Bacterial APA in these environments has been hypothesized to indicate C-limitation of bacterial growth (Hoppe and Ullrich 1999; Nicholson et al. 2006). Elevated APA associated with rapidly sinking particles, subsequent fragmentation and release of surface derived APA to the dissolved phase has also been found to contribute to APA at depth where DIP concentrations are elevated (Koike and Nagata 1997). In addition, non-repressible APA has been found to be a constitutive part of phytoplankton physiology in coastal regions resulting in detectable APA under DIP-replete conditions (Dyhrman and Ruttenberg 2006; Labry et al. 2016). These findings suggest that AP has a variety of roles in the marine P cycle.

AP dynamics in the marine environment can be investigated by hydrolysis rate assay experiments (Ammerman 1993), single cell enzyme labeling (Dyhrman and Palenik 1999), or identification of the presence and expression of genes encoding for AP (e.g., Orchard et al. 2009). Enzyme kinetics are derived from hydrolysis rate assay experiments and are used to characterize the maximum potential rate of reaction, V_{max}, and the inverse of the enzyme affinity for a substrate, K_m (Table 1). Enzyme labeled fluorescence (ELF-97; Dyhrman and Palenik 1999) allows identification of the individual cells responsible for APA through staining the active site of the enzyme with an insoluble precipitate upon hydrolysis. More recently, genomics have been used to identify genes that code for AP synthesis (phoA, phoX, and phoD) in various phytoplankton species and marine bacteria to investigate the distribution and regulation of AP in the marine environment (Orchard et al. 2009; Sebastian and Ammerman 2009). In the advent of these various techniques, interrogating the biogeochemical function and role of AP in the marine environment and challenging traditional paradigms of DIP-limitation have become of key interest to better understanding the significance of this enzyme in the marine P cycle.

Studies on AP and its importance in P cycling in the shallow (< 200 m) shelf sea environment are relatively limited considering the significance of such regions in global biogeochemical cycles. Shelf seas cover 7% of the global ocean by area, yet contribute up to 30% of ocean primary productivity

and 20% of organic matter production (Barrón and Duarte 2015). Therefore, better constraining how nutrients are cycled in the water column in shelf sea regions is important to understanding both the adjacent basin scale and global nutrient cycles. In this study, our aim was to characterize APA in the DIP-replete temperate, seasonally stratified Celtic Sea, part of the Northwest European shelf. We report multi-year summertime vertical distributions of AP rates and kinetics. Our findings add to the cumulating body of evidence on APA in DIP-replete marine environments. Using new insights from novel particle segregation experiments, our study emphasizes the role of sinking particles in vertical distribution of AP-facilitated remineralization of OP and speculates on the drivers and consequences of enhanced particle associated APA.

Materials and methods

Sample collection

Samples were collected in the seasonally stratified temperate Celtic Sea (*see* Davis et al. 2014; approximately 50°N, 8°W) during July 2008 (RRS James Cook, JC025), June 2010 (RRS Discovery, D352), and July 2014 (RRS Discovery, DY026). Samples were collected throughout the water column using a rosette frame, supporting a Seabird 911 conductivity, depth, temperature (CTD) instrument, calibrated fluorometer and 20-liter Niskin bottles. For dissolved constituents, seawater samples were filtered through a Whatman glass fiber filter (GF/F, 0.7 μm pore size, precombusted at 450°C for 4 h prior to acid washing, deionized water rinsing and drying at 50°C) and stored in acid-washed 175 mL or 250 mL HDPE bottles at −20°C until analysis. Samples for particulate phosphorus (PPhos) analysis were collected by filtering 1 L of seawater under low vacuum pressure (< 12 kPa) onto pre-combusted GF/Fs (treatment as above). Samples were stored at −20°C until analysis. Total APA was determined using unfiltered seawater from the CTD.

Marine snow catcher deployments

The marine snow catcher (MSC) is a large (95 L) bottle that acts as a settling column by collecting water from depth and consequently segregating particles based on their sinking rates during a 2 h settling period. Particle fractions are arbitrarily classified as suspended in the upper 10 L (F_{susp}) and slow sinking in the bottom 7 L (F_{slow}), with fast sinking particles collecting on the base tray (F_{fast}; Riley et al. 2012; Cavan et al. 2014). The MSC was deployed below the thermocline to 65 m and three particle fractions were sampled in triplicate for APA (fixed concentration substrate addition) to quantify particle associated APA. The MSC concentrated F_{fast} and F_{slow} by a factor of 95-fold and 13.5-fold, respectively, providing a means to reliably measure APA associated with F_{fast} and F_{slow} at a level that was detectable above the background signal associated with F_{susp}, which included the dissolved phase (*see* below).

Chlorophyll *a*

Chlorophyll *a* (Chl *a*) fluorescence data from the CTD mounted fluorometer were calibrated for each cruise following linear regression with Chl *a* concentrations determined from seawater samples. Samples were filtered onto Fisherbrand MF300 filters (25 mm diameter, 0.7 μm effective pore size) and extracted in 8 mL of 90% acetone for 20 h and the resulting Chl *a* fluorescence was measured using a Turner Trilogy fluorometer calibrated with a solid standard and Chl *a* extract (Sigma Aldrich; Davidson et al. 2013).

Dissolved nutrients

Dissolved inorganic phosphorus (DIP) concentrations were determined in triplicate by the molybdenum blue method (Murphy and Riley 1962) using a Bran and Leubbe QuAAtro 5-channel autoanalyser (DIP detection limit 50 nM). At low DIP concentrations (< 100 nM), samples were reanalyzed in triplicate 50 mL aliquots using the magnesium induced co-precipitation method (Karl and Tien 1992) prior to DIP determination as above (detection limit 20 nM DIP).

UV-hydrolysable total dissolved phosphorus (TDP) was determined by UV oxidation of 10 mL of seawater sample in triplicate at 82°C for 2 h using a Metrohm 705 UV oxidizer (Armstrong et al. 1966). DOP was quantified by the difference in DIP concentrations before and after UV oxidation (i.e., DOP = TDP − DIP; DOP detection limit 40 nM).

To estimate the AP-hydrolysable fraction of the DOP pool, phosphomonoester (PME) concentrations were determined by incubating samples in triplicate with a commercially available AP isolated from *Escherichia coli* (Sigma Aldrich), following Monbet et al. (2007). Filtered seawater samples (Millipore polyethene membrane filter, 0.2 μm pore size, 47 mm diameter; under low vacuum pressure, < 12 kPa) were incubated in triplicate 25 mL aliquots, plus two blanks, in Sterelins (Fisherbrand). An AP solution was prepared in 0.1 M Tris buffer (pH 9) solution to a final concentration of 1 unit mL^{-1} with magnesium chloride (final concentration 2 μM $MgCl_2$) as an enzyme activator. Samples were spiked with enzyme solution (5% vol : vol) and incubated at ~ 18°C for 20 h in the dark. DIP was analyzed in the controls and samples as above. PME was quantified as the difference in DIP concentration between control and sample ($PME = DIP_{sample} - DIP_{control}$). To check analytical accuracy and monitor potential inter-analysis variability, triplicate solutions of a model compound (1 μM D-glucose 6-phosphate dipotassium salt hydrate, Sigma Aldrich) were incubated and analyzed with each experiment. Mean recovery of the model compound during the analysis period was 99.7% ± 2.1% ($n = 18$).

Particulate nutrient analysis

Total PPhos concentrations were determined by acid hydrolysis (Karl et al. 1991). Briefly, samples were combusted (450°C, 4.5 h) prior to acid hydrolysis (5 mL of 0.5 M HCl;

VWR Analytical Grade) and sonication (60 min), followed by centrifugation (3000 × *g*, 30 min) and subsequent determination of DIP (as above) in the diluted supernatant. To check analytical accuracy and monitor potential inter-analysis variability, a certified reference material (NIST Apple Leaves 1515, 0.159% P by weight) was analyzed in triplicate with each run. Mean recovery of the reference material during the analysis period was 98.5% ± 3.9% ($n = 24$).

Particulate organic carbon (POC) concentrations were determined by filtering 2 L of seawater onto a Whatman glass fiber filter (GF/F, 0.7 μm pore size, 25 mm diameter, precombusted at 450°C for 4 h). POC was analyzed after vapor phase decarbonation using a Carlo Erba Elemental Analyzer (Yamamuro and Kayanne 1995).

APA

Total APA was measured in unfiltered seawater samples from the CTD using the synthetic fluorogenic substrate 4-methylumbeliferyll-phosphate (MUFP, Sigma Aldrich), as described in Ammerman (1993). Stock solutions of MUFP at 100 mM in 2-methoxyethanol were prepared and subsequently diluted with deionized water to make a 100 μM stock prior to each experiment. In brief, 250 mL of seawater was incubated in polycarbonate bottles in triplicate in on-deck incubators at adjusted light levels and sea surface temperature with MUFP to a fixed final concentration of 1200 nM MUFP or final concentration ranging from 200 nM to 2000 nM MUFP. Particle fractions from the MSC were incubated in the dark at 10°C to simulate in situ temperature and light conditions. Hydrolysis of MUFP to the fluorescent product, 4-methylumbelliferone (MUF) was measured every 2 h for 16 h using a Turner 10Au fluorometer (365 nm excitation, 455 nm emission) after addition of a buffer solution (3 : 1 sample: 50 mM sodium tetraborate solution, pH 10.5). A linear calibration was produced daily using MUF standards (concentration range 0–2000 nM) and was used to convert the rate of change in fluorescence to MUFP hydrolysis rate, here considered to be synonymous with volumetric APA (APA_{VOL}, nM P h^{-1}). Fluorescence measurements were corrected for seawater blanks, and rates were corrected for abiotic MUFP hydrolysis or degradation using blanks (deionized water plus 800 nM MUFP; boiled sample plus 800 nM MUFP). Blanks and controls showed no significant change in fluorescence over time.

Enzyme kinetic parameters were determined using data from incubation of seawater with variable concentrations of MUFP (200–2000 nM MUFP). Estimation of Michaelis-Menten parameters of APA was performed using transformations of the Michaelis-Menten equation to produce substrate-response curves or linear regression plots. Eadie-Hofstee (e.g., Gambin et al. 1999), Hanes-Woolf (e.g., Duhamel et al. 2011), and Lineweaver-Burk (e.g., Rengefors et al. 2003) plots are three commonly used transformation plots. Here, the maximum hydrolysis rates (V_{max}) and half saturation constant (K_m) were determined using the Hanes-Woolf plot graphical linearization of the Michaelis-Menten equation following Duhamel et al. (2011). The K_m values estimated correspond to the affinity of the natural consortium of enzymes sampled for the artificial substrate added (MUFP). Note that enzyme activity is typically subject to inhibition with natural substrates (e.g., PME) already present in the sample.

Ideally, hydrolysis rates are normalized to enzyme concentration (Suzumura et al. 2012). However, in natural samples, this is often unknown and difficult to quantify. Therefore, in practice, APA is normalized to biomass through available parameters such as Chl *a* (Mahaffey et al. 2014), C (Mather et al. 2008), and cell abundance (Duhamel et al. 2011). As this study was focused on the distribution and rate of AP-facilitated P cycling in the water column and the potential mechanisms governing its distribution, we present data as volumetric rates, APA_{VOL}. To investigate the potential mechanisms driving trends in APA_{VOL}, total APA was normalized to Chl *a* for autotrophs, POC as a proxy for total C biomass, and bacterial abundance (data provided by S. McNeil, Scottish Marine Association).

Segregation of particle-associated APA

APA was determined in three fractions sampled from the MSC to assess whether sinking particles behaved as a vehicle for transferring AP through the water column. These fractions were defined as F_{susp}, which corresponds to the dissolved phase and suspended particle fraction, F_{slow}, which corresponds to slow sinking particle fraction and F_{fast}, which corresponds to fast sinking particle fraction. F_{fast} was collected on a removable base tray separated into quarters. Each fraction was incubated in triplicate with a single MUFP addition (1200 nM) plus a blank, and APA was determined as above. Given the small volume of the base tray unit, F_{fast} was divided into equal aliquots that were each resuspended in 250 mL of sample from F_{susp} to provide sufficient volume for replicate APA incubations and blanks. Fraction-specific APA for F_{slow} and F_{fast} were corrected to account for the measured contribution of APA from F_{susp}. Thus AP rates of F_{susp} were subtracted from the APA measured in F_{slow} and F_{fast}, resulting in F_{susp} corrected rates termed $F_{slow\text{-}susp}$ and $F_{fast\text{-}susp}$, respectively. To quantify the contribution of each particle fraction (F_{susp}, $F_{slow\text{-}susp}$, $F_{fast\text{-}susp}$) to total APA in the water column, the rates of APA in concentrated samples were normalized to the volume associated with each particle fraction in the MSC (7 L for $F_{slow\text{-}susp}$, 95 L for the $F_{fast\text{-}susp}$) relative to the volume of the MSC (95 L; *see* Cavan et al. 2014).

Cell-specific APA

Cell-specific enzyme-labelled fluorescence (APA_{ELF}) was measured during June 2010 (D352). In brief, particles were concentrated by filtration of 1 L of seawater sample onto a polycarbonate filter (0.8 μm pore size, 25 mm diameter, Durapore) under low vacuum pressure (< 12 kPa) without drying, as described by Rees et al. (2009). Thereafter, the

method was as described by Dyhrman and Palenik (1999) using ELF-97 reagents (Molecular Probes). Samples were stored in the dark at 4°C until analysis (within 14 d) using a Zeiss epifluorescence microscope with a 4′6-diaminidino-2-phenylindole (DAPI) long pass filter set (emission 520 nm, excitation 350 nm). Cell abundance analysis of ELF labelling was not conducted as labelled particles were too varied in size and form to provide reliable quantification of their nature and origin.

Bacterial abundance and productivity

Bacterial abundance and bacterial production (BP) data were provided by K. Davidson and S. McNeil of the Scottish Marine Association (Davidson et al. 2013, unpubl.). Bacterial abundance was determined as described in Davidson et al. (2007). In brief, 5 mL of sample was stained for 5 min with 5 μg mL^{-1} DAPI, filtered onto a black 0.2 μm × 25 mm diameter polycarbonate filter (with 0.2 μm cellulose nitrate backing filter), washed with 0.2-μm-filtered deionized water, mounted on a slide, and stored frozen at −20°C prior to analysis at ×1000 magnification under fluorescence illumination using a Zeiss Axiovert 100 microscope equipped with 09 (blue excitation) and 02 (ultraviolet excitation) filter blocks (Davidson et al. 2007). Bacterial productivity was assayed as described in Davidson et al. (2013), using the micro-centrifuge method (Kirchman 2001) with [^{3}H]-Thymidine or [^{14}C]-Leucine additions (Davidson et al. 2013).

Statistical analysis

For replicate analysis or incubation, the mean ± 1 SD was calculated and is reported here. Statistical analysis was performed using SigmaStat in the SigmaPlot 13.0 software package (Systat Software). Statistical analyses comparing paired groups of data were performed using the Mann Whitney test, with significance detected if p was less than 0.05.

Results

Samples were collected in the central Celtic Sea region (approximately 50°N, 8°W) in July 2008 (JC025), June 2010 (D352), and August 2014 (DY026). Unlike the open ocean, where the water column is permanently stratified and vertically stable, wind and tidal driven mixing act to alter the vertical structure of the water column in a shelf sea on timescales of hours to days. This creates a highly dynamic, physically variable environment which impacts the distribution of biogeochemical properties and processes.

During this study, the water column was strongly stratified throughout each sampling campaign, with summertime production dominated by the subsurface chlorophyll maximum (SCM; Hickman et al. 2012; Williams et al. 2013; Davis et al. 2014). Temperature in the bottom mixed layer (BML, 9.7–10.5°C) and surface mixed layer (SML, 14.4–16.6°C) were comparable between years (Fig. 1A), with the greatest variability in SML temperatures occurring during JC025 (14.4–16.0°C, Fig. 1A) due to a storm (Davis et al. 2014). The depth of the base of the thermocline, defined as a deviation in temperature of > 0.05°C from the bottom temperature, varied between 35 m and 50 m (Fig. 1A). This was typical for this region during seasonal stratification due to variability in tide and wind induced mixing at the thermocline and the influence of migrating internal waves moving the thermocline vertically (Sharples et al. 2009; Williams et al. 2013). These processes also contribute to characteristic patchiness of SCM on both spatial and temporal scales linked with the variability of small scale turbulent mixing at the thermocline (Sharples et al. 2007; Tweddle et al. 2013).

A persistent SCM was observed during all sampling campaigns at a depth between 30 m and 50 m (< 1.8 μg L^{-1}; Fig. 1B), while PPhos concentrations were highest in the upper 20 m (0.02–0.20 μM; Fig. 1C). PPhos and Chl *a* maxima often occur at different depths to one another in shelf sea environments due to photo-quenching of Chl *a* near the surface, photo-acclimation of phytoplankton (Moore et al. 2006), and vertical gradients in phytoplankton community composition in the subsurface Chl *a* maximum (Hickman et al. 2009). Below the thermocline in the BML, Chl *a* and PPhos concentrations were significantly lower (mean ± SD, 0.08 ± 0.01 μg L^{-1}, $n = 536$ and 0.02 ± 0.03 μM, $n = 26$, respectively; Fig. 1B,C) than above the base of the thermocline in the SML ($p < 0.001$).

Mean (± SD) DIP concentrations in the top 20 m (0.08 ± 0.03 μM, $n = 45$; from 0.03 μM to 0.16 μM; Fig. 1D) were eight times lower than observed in the BML where the mean concentration was 0.66 ± 0.06 μM (from 0.54 μM to 0.77 μM; $n = 36$; $p < 0.001$; Fig. 1D). The phosphocline was situated in the lower thermocline between 30 m and 50 m (Fig. 1A,D) and was coupled with depth of the SCM (Fig. 1B). Inclusion of the phosphocline in the SML still resulted in DIP concentrations being significantly lower (0.23 ± 0.21 μM) in the SML relative to the BML (0.66 ± 0.06 μM; $p < 0.001$).

Mean DOP and PME concentrations in the SML were significantly higher (0.17 ± 0.05 μM and 0.06 ± 0.04 μM, respectively) compared to the BML (0.13 ± 0.06 μM and 0.02 ± 0.03 μM, respectively; $p = 0.014$ and $p < 0.001$, Fig. 1E,F, respectively). The DOP pool accounted for 51 ± 20% ($n = 103$) of the TDP pool in the SML and 18 ± 5% ($n = 38$) in the BML. PME represented 38 ± 50% of DOP in the SML ($n = 60$) and 21 ± 43% ($n = 18$) of DOP in the BML (Fig. 1E,F).

Total volumetric rates of APA (APA_{VOL}) were determined for unfiltered water column samples collected from 16 CTD casts (eight in July 2008, seven in June 2010, and one in early August 2014) between 0 m and 75 m depth ($n = 45$; Fig. 2) and were significantly higher in the BML than the SML (0.93 ± 0.32 nM P h^{-1} and 0.30 ± 0.24 nM P h^{-1}, respectively, $p < 0.001$). Measured discrete APA_{VOL} ranged from 0.01 nM P h^{-1} at 5 m to 1.54 nM P h^{-1} at 55 m. Discrete data were subsequently grouped into seven 10 m-depth bins ($n = 45$, Fig. 2A). To account for vertical change in biomass

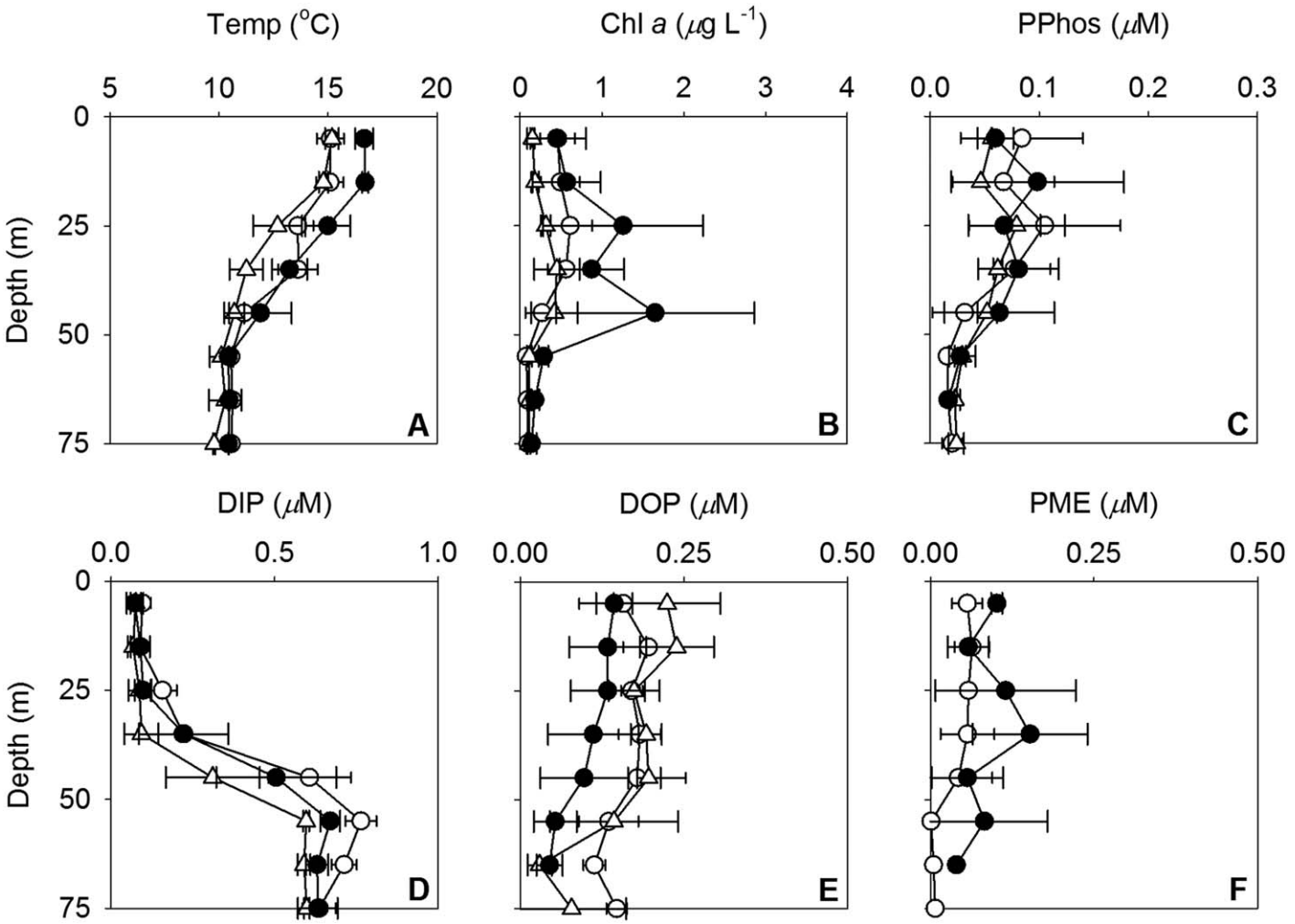

Fig. 1. Depth binned (10 m) profiles (± 1 s.d.) of (**A**) temperature (Temp, °C), (**B**) Chl *a* (μg L^{-1}), (**C**) PPhos (μM), (**D**) DIP (μM), (**E**) DOP (μM), (**F**) PME (μM) from July 2008 (JC025; closed circles), June 2010 (D352; open circles), and August 2014 (DY026; open triangles). DIP, DOP, and PME samples were analyzed in triplicate and data were rejected if the standard deviation was greater than 5% of the mean value.

in the water column, APA was normalized to Chl *a* as a proxy for autotrophs ($APA_{Chl\ a}$, Fig. 2D), POC to account for total C biomass (APA_{POC}, Fig. 2G) and bacterial abundance (APA_{BA}, Fig. 2J). Biomass normalized APA was also positively correlated with depth ($APA_{Chl\ a}$ $r^2 = 0.34$, $p < 0.001$; APA_{POC} $r^2 = 0.34$, $p < 0.001$; and APA_{BA} $r^2 = 0.50$, $p < 0.001$, data not shown) and normalized rates were significantly higher in the BML than in the SML (APA_{VOL} $p = 0.024$, $APA_{Chl\ a}$ $p < 0.001$, APA_{POC} and APA_{BA} $p = 0.002$).

Kinetic parameters of APA were assessed between 0 m and 75 m and data were subsequently grouped into six 10 m-depth bins ($n = 30$; Fig. 2). The maximum rate of MUFP hydrolysis, V_{max}, is presented as a volumetric rate (V_{maxVOL}, Fig. 2B), Chl *a* normalized ($V_{maxChl\ a}$, Fig. 2E), POC normalized (V_{maxPOC}, Fig. 2H) and bacterial abundance normalized (V_{maxBA}, Fig. 2K) rates. V_{maxVOL} was six times lower at 5 m (0.24 ± 0.15 nM P h^{-1}) compared to 45 m (1.45 ± 0.62 nM P h^{-1}; Fig. 2B).

K_m is defined as the inverse of the affinity of the natural consortium of enzymes for the synthetic substrate, in this case, MUFP. As the natural enzyme concentration was unknown, K_m was normalized to the same biomass proxies as APA and V_{max} (Fig. 2C,F,I,L). K_{mVOL} (nM P; Fig. 2C) was more variable in the SML (from 34 nM P to 3143 nM P) than in the BML (from 311 nM P to 1136 nM P). Volumetric and biomass normalized K_m values were also highly variable, resulting in no significant difference between K_m in the SML and BML for K_{mVOL} and K_{mBA} (385 ± 740 nM, 633 ± 316 nM, $p = 0.77$; and 62 ± 56 nmol P 10^8 cell^{-1}, 101 ± 38 nmol P 10^8 cell^{-1}, $p = 0.053$, respectively), but a significant difference between $K_{mChl\ a}$ and K_{mPOC} in the SML (4216 ± 5631 nmol P μg Chl a^{-1} and 148 ± 177 nmol P μmol C^{-1}, respectively) and BML ($11{,}104 \pm 3184$ nmol P μg Chl a^{-1} and 623 ± 639 nmol P μmol C^{-1}; $p = 0.014$ and 0.03 respectively).

Rates of APA_{VOL} were positively correlated with depth ($r^2 = 0.51$, $p < 0.001$; Fig. 3A) and DIP ($r^2 = 0.60$, $p < 0.001$;

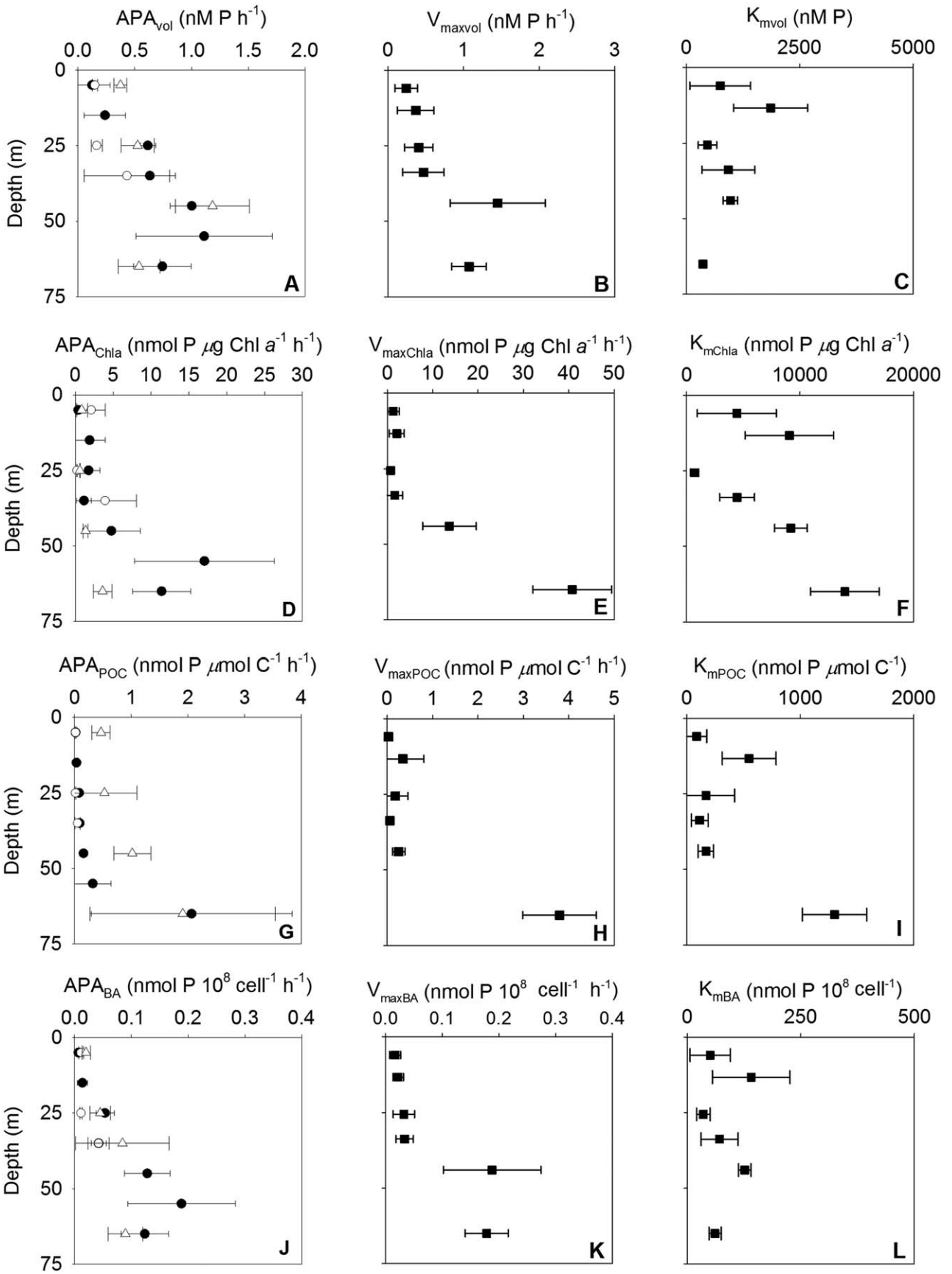

Fig. 2. Depth binned (10 m) profiles (± 1 SD) of volumetric APA (left column; APA_{VOL}, nM P h^{-1}; open circles represent July 2008, closed circles represent June 2010, open triangles represent August 2014), V_{maxVOL} (center column; nM P h^{-1}; closed circles represent all data) and K_{mVOL} (right column; nM P; closed circles represent all data) presented in volumetric (**A**–**C**; nM P h^{-1} or nM P) and rates normalized to Chl *a* (**D**–**F**; nmol P μg Chl a^{-1} h^{-1} or nmol P μg Chl a^{-1}), POC (**G**–**I**; nmol P μmol C $^{-1}$ h^{-1} or nmol P μmol C $^{-1}$), and bacterial abundance (**J**–**L**; nmol P 10^8 $cell^{-1}$ h^{-1} or nmol P 10^8 $cell^{-1}$).

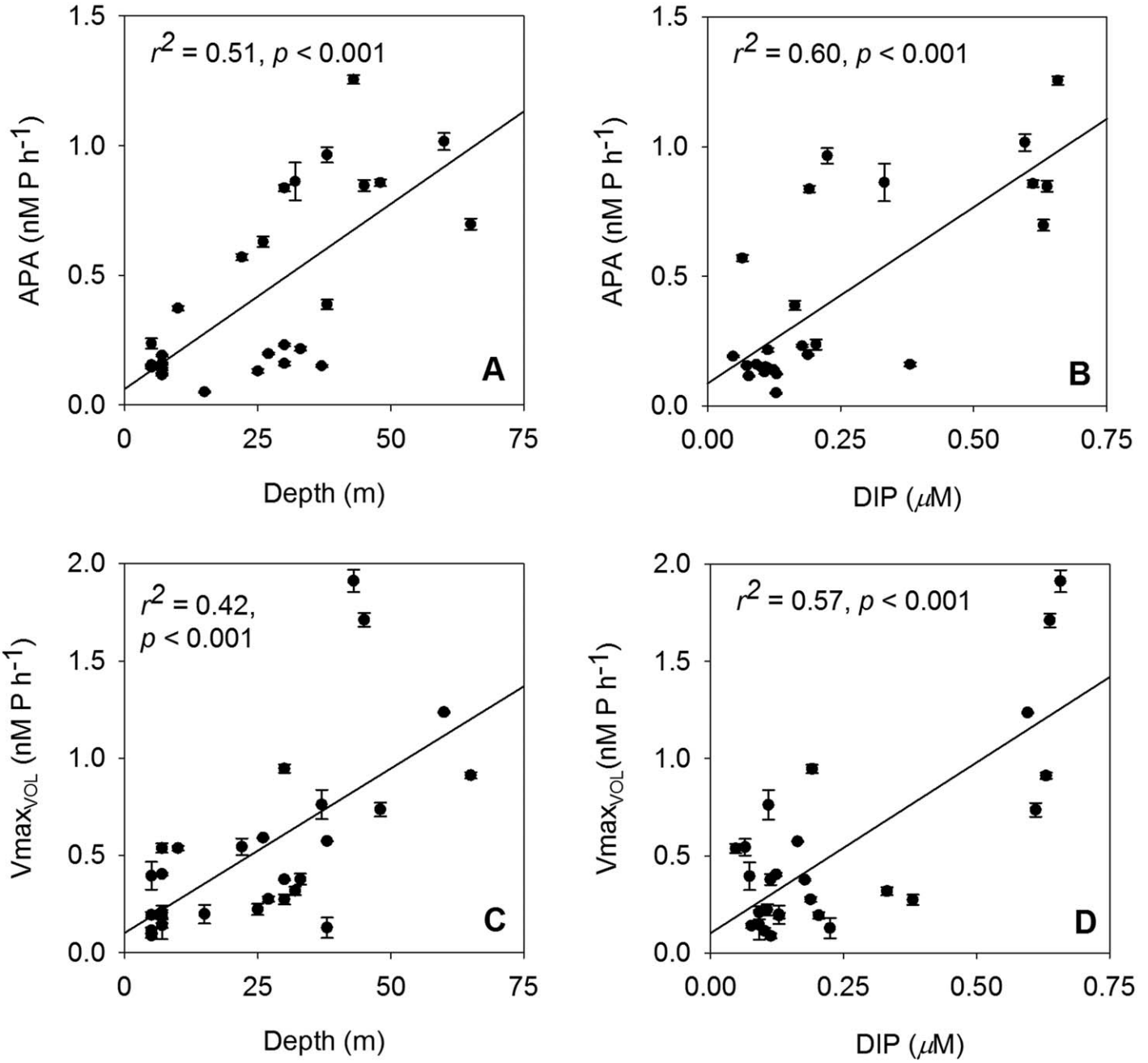

Fig. 3. Linear regression plots of (**A**) APA_{VOL} (± 1 SD; nM P h^{-1}); vs. depth (m), (**B**) APA_{VOL} (± 1 SD; nM P h^{-1}) vs. DIP (μM), (**C**) V_{maxVOL} (± 1 SD; nM P h^{-1}) vs. depth (m), (**D**) V_{maxVOL} (± 1 SD; nM P h^{-1}) vs. DIP (μM). R^2 and p values are displayed.

Fig. 3B). Discrete V_{maxVOL} was positively correlated with depth ($r^2 = 0.42$, $p < 0.001$; Fig. 3C) and DIP ($r^2 = 0.57$, $p < 0.001$; Fig. 3D) and V_{maxVOL} was significantly lower in the SML (0.48 ± 0.44 nM P h^{-1}; $n = 25$) than in the BML (1.07 ± 0.22 nM P h^{-1}, $p = 0.035$; $n = 4$). $V_{maxChl\ a}$ and V_{maxPOC} were positively correlated with depth ($r^2 = 0.48$, $p < 0.001$ and $r^2 = 0.36$, $p < 0.001$, respectively, data not shown). $V_{maxChl\ a}$ and V_{maxPOC} were 15- and 35-times higher in the BML (40.8 ± 8.7 nmol P μg Chl a^{-1} h^{-1} and 3.80 ± 0.81 nmol P μmol C^{-1} h^{-1}, respectively) compared to the SML (2.75 ± 4.5 nmol P μg Chl a^{-1} h^{-1}, $p = 0.009$ and 0.11 ± 0.17 nmol P μmol C^{-1} h^{-1}, $p = 0.016$, respectively).

Particle concentrated APA associated with $F_{fast\text{-}susp}$ (15.41 ± 2.06 nM P h^{-1}) was 20 times higher than F_{susp} (0.76 ± 0.29 nM P h^{-1}) and 53 times higher than $F_{slow\text{-}susp}$ (0.29 ± 0.31 nM P h^{-1}, data not shown), suggesting enhanced APA associated with fast sinking particles relative to slow sinking particles and the dissolved and suspended

Table 2. Summary of results from the MSC.*

Particle fraction	$APA_{VOL} \pm SD$ (nM P h^{-1})	POC ± SD (μM)	BP (nM C h^{-1})	$APA_{POC} \pm SD$ (nmol P μmol C^{-1} h^{-1})	$APA_{BP} \pm SD$ (nmol P nmol C^{-1})
F_{susp}	0.76 ± 0.29	5.79 ± 0.90	1.04	0.13 ± 0.05	0.73 ± 0.3
$F_{slow\text{-}susp}$	0.02 ± 0.02	0.34 ± 0.03	0.19	0.06 ± 0.07	0.11 ± 0.12
$F_{fast\text{-}susp}$	0.16 ± 0.02	0.21 ± 0.03	0.01	0.76 ± 0.10	21.1 ± 2.2

* Note: Abbreviations denote APA rate (APA_{VOL}, ± 1 SD, nM P h^{-1}), POC (± 1 SD, μM), BP (nM C h^{-1}, data provided by S. McNeil, Scottish Marine Association), POC normalized APA (APA_{POC}, ± 1 SD, nmol P μmol C^{-1} h^{-1}), BP normalized APA (APA_{BP}, ± 1 SD, nmol P mol C^{-1}) for dissolved and suspended (F_{susp}), slow sinking ($F_{slow\text{-}susp}$), and fast sinking ($F_{fast\text{-}susp}$) particle fractions.

fraction. When these APA rate measurements were corrected for the concentration factor incurred during particle segregation and concentration in the MSC, AP rates in the $F_{fast\text{-}susp}$ (0.16 ± 0.02 nM P h^{-1}) were five times lower than the APA of F_{susp} (0.76 ± 0.29 nM P h^{-1}; Table 2) but were eight times higher than APA associated with $F_{slow\text{-}susp}$ (0.02 ± 0.02 nM P h^{-1}; Table 2). Thus, $F_{fast\text{-}susp}$ represented 17% ± 3% of APA measured from the MSC compared to F_{susp} and $F_{slow\text{-}susp}$ combined, which represented 81% ± 43% and 2% ± 3%, respectively. By contrast, POC in $F_{fast\text{-}susp}$ represented only 3% ± 0.7% of total POC, whereas $F_{slow\text{-}susp}$ and F_{susp} represented 5% ± 0.7% and 91% ± 20% of total POC, respectively (Table 2). Rates of BP were highest in F_{susp} (1.04 nM C h^{-1}), with rates in the $F_{slow\text{-}susp}$ (0.19 nM C h^{-1}) and $F_{fast\text{-}susp}$ (0.01 nM C h^{-1}) accounting for only 16% and 1% of total BP, respectively (Table 2).

When APA_{VOL} associated with these different fractions was normalized to POC and BP (Table 2), APA_{POC} and APA_{BP} were higher in $F_{fast\text{-}susp}$ (0.76 ± 0.10 nmol P μmol C^{-1} h^{-1} and 21.13 ± 2.2 nmol P nmol C^{-1}, respectively) than F_{susp} (0.13 ± 0.05 nmol P μmol C^{-1} h^{-1} and 0.73 ± 0.3 nmol P nmol C^{-1}, respectively) and $F_{slow\text{-}susp}$ (0.06 ± 0.07 nmol P μmol C^{-1} h^{-1} and 0.11 ± 0.12 nmol P nmol C^{-1}, respectively; Table 2). Enzyme labelled fluorescence (APA_{ELF}), used to qualitatively assess particle-specific APA (for particles > 0.8 μm), indicated that particle-associated APA was predominantly linked to detrital particles rather than ELF-active phytoplankton cells (Fig. 4). Microscopic analysis revealed that fast sinking particles from the MSC were relatively large phyto-detritus aggregates or zooplankton faecal pellets, while $F_{slow\text{-}susp}$ constituted smaller, less dense phytodetritus and very small aggregates (Cavan unpubl.).

Discussion

Role of APA in the marine environment

In the surface waters of the open ocean, the presence of elevated APA in DIP deplete (< 30 nM) regions is typically interpreted as being indicative of DIP-limitation (Mahaffey et al. 2014) or P stress (Suzumura et al. 2012). In the current shelf sea study, DIP concentrations ranged from 30 nM to 770 nM and the mean rate of APA was 10 ± 9 nM P d^{-1} (mean ± SD). Using the database of Mahaffey et al. (2014) to assess APA rates over the same DIP concentration range in the open ocean, the equivalent mean rate of APA is 11 ± 19 nM P d^{-1}, which is comparable with this study (Table 1). While the rates of APA are of similar magnitude over the same range of DIP concentrations in these contrasting environments, it is their relationship to environmental variables and therefore the function of AP that differs in the shelf sea environment. In contrast to subtropical open ocean studies, where there is an inverse hyperbolic relationship between APA and DIP (Mahaffey et al. 2014), APA had a positive linear correlation with DIP and depth (Fig. 3) in this shelf sea study. Our findings suggest that APA in this shallow shelf sea environment was not induced simply in response to DIP-limitation or P stress of the microbial community. Instead, our data strongly support the cumulating body of evidence that APA has a potentially ubiquitous and important role in OP remineralization through the water column.

The role of sinking particles

In this study, we observed a significant increase in total APA and V_{max} with depth. Here, we focus on potential explanations for this observation and implications for water column P cycling. Segregation of particles based on sinking speed indicated that APA was strongly concentrated in $F_{fast\text{-}susp}$ relative to other biogeochemical parameters (i.e., POC and BP), and that this same concentration effect was not observed for $F_{slow\text{-}susp}$ or F_{susp}. For example, $F_{fast\text{-}susp}$ contributed 17% ± 3% of total APA while contributing only 3% ± 0.7% of total POC, whereas F_{susp} represented 81% ± 43% of APA and 91% ± 20% of POC. Furthermore, APA_{POC} and APA_{BP} associated with $F_{fast\text{-}susp}$ were fourfold and 25-fold higher compared to F_{susp} and $F_{slow\text{-}susp}$ combined (Table 2). APA_{VOL}, APA_{POC}, and APA_{BP} were 8-, 13-, and 192-fold higher in the $F_{fast\text{-}susp}$ compared to the $F_{slow\text{-}susp}$ (Table 2), highlighting that fast sinking particles were hotspots for APA relative to biomass proxies.

The origin of $F_{fast\text{-}susp}$ was predominantly faecal material, while particles in $F_{slow\text{-}susp}$ were typically smaller, less dense phytodetritus and very small aggregates that did not sink as rapidly (Cavan et al. unpubl.). As autotrophic biomass in the surface layer is a key source of phytodetritus and slow

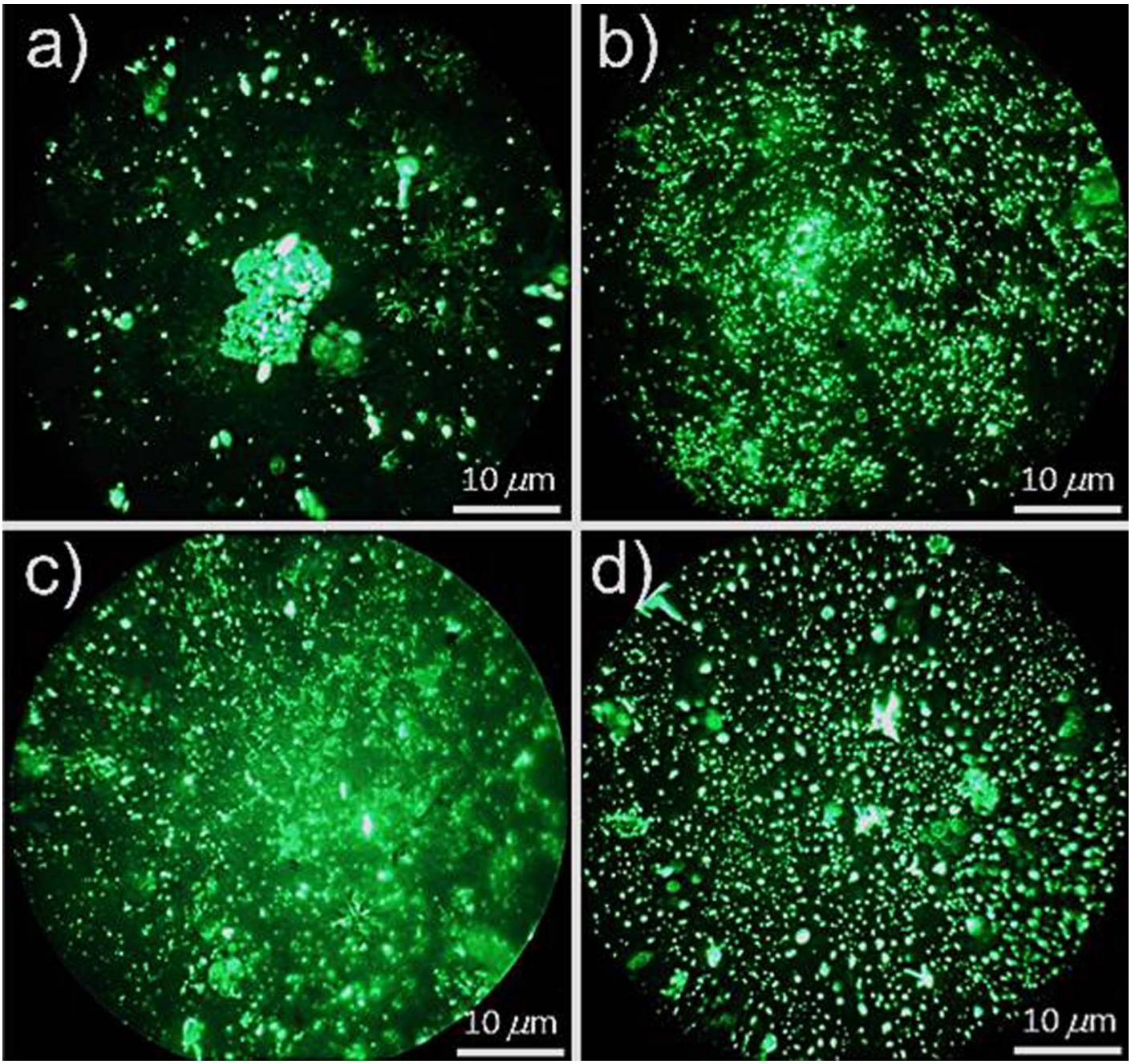

Fig. 4. Example epifluorescence images with a DAPI long-pass filter set of enzyme labelled fluorescence (APA_{ELF})-assayed samples collected during D352 from (**A**) surface, (**B**) subsurface chlorophyll maxima peak, (**C**) base or downslope of the subsurface chlorophyll maxima, (**D**) below the thermocline or BML. Field of view diameter is 50 μm.

sinking material (Cavan et al. 2014), it is probable that the origin of APA associated with $F_{\text{slow-susp}}$ reflects the low APA observed above the base of the thermocline. In contrast, the primary source of $F_{\text{fast-susp}}$ was faecal material, and therefore, there was potentially a different source and depth of source of AP associated with this particle fraction.

Disaggregation of fast sinking particles as they sink through the water column has the potential to increase the surface area which bacteria can colonize (Kirchman 1993), while not necessarily affecting the density or sinking rate of those particles. Bacteria attached to particles have a higher cell-specific ectoprotease activity compared to free-living bacteria (Hoppe et al. 1988; Karner and Herndl 1992; Grossart et al. 2007). Enhanced hydrolytic enzyme activity on particles collected from a macrotidal estuary (Labry et al. 2016) and from the Southern California Bight (Smith et al. 1992)

has been previously reported but these observations were focused on surface waters only (< 25 m). Our study shows that significant hydrolytic enzyme activity on particle surfaces is observed in the dark, DIP-replete bottom waters of a shelf sea. Thus, we postulate that the increase in APA with depth may be linked to transport to depth associated with fast sinking particles and/or release of APA from particles during disaggregation accompanied by higher activity associated with particle-bound bacteria.

The role of bacteria and potential decoupling of nutrient remineralization

Relative to typical whole water BP rates in this shelf sea environment ($\sim$ 15–50 nM C h^{-1}; Davidson et al. 2013), total BP associated with particle fractions was low (1.24 nM C h^{-1}), with rates of BP associated with $F_{\text{slow-susp}}$ and $F_{\text{sink-susp}}$ representing only 14% and 1% of BP measured from the MSC (Table 2), implying that the bacterial C assimilation associated with particulate matter, especially $F_{\text{fast-susp}}$, was low (Table 2). Comparing BP with APA, mean AP rates are eightfold higher on $F_{\text{fast-susp}}$ compared to $F_{\text{slow-susp}}$, whereas particle associated BP on $F_{\text{fast-susp}}$ is only 5% of BP associated with $F_{\text{slow-susp}}$ (Table 2). While we have not accounted for bacterial respiration on particles, this finding suggests that there is decoupling between hydrolytic enzyme activity and bacterial C consumption on fast sinking particle surfaces. If BP represents some fraction of particle C remineralization, then our results suggest that P was preferentially remineralized relative to C on fast sinking particles.

Similar observations have been observed for C and N on particle aggregates in the Southern California Bight. Smith et al. (1992) measured a low bacterial carbon demand (BCD) on particle aggregates of > 0.5 mm but protease activity (i.e., solubilization of N) was 1–3 orders of magnitude higher than glucosidase activity (i.e., solubilization of C), providing a biochemical mechanism for preferential remineralization of N relative to C. Our findings provide evidence for preferential remineralization of P relative to C associated with fast sinking particles below the thermocline. To provide an accurate estimate of the C : P stoichiometry of remineralization, BCD and change in particulate C : N : P during incubations would need to be measured alongside APA.

There are a number of possible explanations for enhanced APA relative to C acquisition on particles. Bacteria may produce AP to meet their P demands during intense growth (Luo et al. 2009) or to access the organic C moiety (Hoppe and Ullrich 1999; Nicholson et al. 2006). Elevated APA or $V_{\max}$ in high DIP waters, either at depth or in coastal regions, has been observed in the Indian Ocean (Hoppe and Ullrich 1999), the North and Central Pacific (Koike and Nagata 1997; Duhamel et al. 2011), Central Atlantic Ocean (Baltar et al. 2010), Mediterranean Sea (Tamburini et al. 2009), and San Franciso Bay (Nicholson et al. 2006). In these studies, elevated APA at depth was attributed to bacterially-derived AP either freely dissolved (Hoppe and Ullrich 1999; Duhamel et al. 2011), or associated with colloids or larger particles (Koike and Nagata 1997; Baltar et al. 2010) in response to organic C limitation of bacterial communities either in situ (Hoppe and Ullrich 1999; Nicholson et al. 2006) or transferred from the euphotic layer associated with sinking particles (Koike and Nagata 1997; Colman et al. 2005). This study also found that APA was likely transferred to depth associated with fast sinking particles. However, the origin of the elevated APA associated with F_{fast} in this study remains unclear as surface layer microbial populations were not DIP-limited and rates of APA were low in the surface (0.01 nM P h^{-1} at 5 m).

The role of zooplankton in APA

Fast sinking particles commonly originate from zooplankton faecal pellet excretion (Cavan et al. 2014). APA is associated with zooplankton, both within their body tissue and released during excretion associated with faecal pellets (Jansson 1976; Boavida and Heath 1984) and the freely dissolved phase (Jamet and Boge 1998). During daylight hours in the stratified Celtic Sea zooplankton biomass is concentrated below the thermocline between 60 m and 80 m (Williams 1985; Conway and Williams 1986). The Celtic Sea is DIP-replete relative to N (Pemberton et al. 2004) and under DIP-replete conditions, zooplankton excrete more APA associated with faecal matter reflecting free-AP, rather than membrane-bound AP, in their digestive tracts (McCarthy et al. 2010; Tang et al. 2011). Therefore, we hypothesize that zooplankton may contribute to a mid-water column source of AP via introduction of AP associated with faecal pellets, potentially explaining our observations of increased APA with depth and enhanced APA associated with $F_{\text{fast-susp}}$.

Zooplankton may also release intercellular and internally bound AP to the water column during grazing via fragmentation of phytoplankton cells or aggregates. However, in this study, the latter process seems unlikely to have significantly contributed to the depth distribution of APA given the low APA observed in the surface layer and the low APA associated with $F_{\text{slow-susp}}$, which primarily constituted phytodetritus. In each instance, the AP released to the dissolved phase may be of a constitutive and non-DIP repressible nature (Dyhrman and Ruttenberg 2006; Tamburini et al. 2009).

Implications for P cycling

Whether the mechanism involves enhanced particle associated APA, release of AP from fast sinking particles during fragmentation or association with zooplankton feeding and excretion, the association of AP with particles at depth and potential release of AP to the dissolved phase has significant implications for the marine P cycle. DIP in the deep ocean is derived from two sources: preformed DIP that is advected to depth from surface waters, and regenerated DIP released from the hydrolysis of particulate organic matter, involving a DOP intermediate (Colman et al. 2005). The two processes

are commonly distinguished from one another using apparent oxygen utilization (AOU) to calculate the fraction of the DIP pool that is regenerated through respiration. Decoupling of phosphohydrolytic enzyme activity from bacterial consumption of C will distort the relationship between DIP release from OP and consumption of oxygen via respiration, causing deviations from the assumed P : O_2 stoichiometry required to estimate regenerated P (Anderson and Sarmiento 1995). In this instance, using AOU would lead to an underestimation of regenerated DIP, and thus an overestimate of preformed DIP associated with deep-water formation. Therefore, approaches combining methods such as the oxygen isotopic composition of phosphate with full depth characterization of hydrolytic P enzymes are important in determining remineralization rates of particulate and dissolved organic P in the deep ocean and improve our understanding of the marine P cycle.

Conclusions

In summary, we observed a significant increase in APA and V_{max} with depth and with DIP concentration in a DIP-replete shelf sea environment. APA and V_{max} were significantly higher in the BML than the SML. This difference did not correlate with other measured biogeochemical parameters (Chl *a*, POC, BA), suggesting that the distribution of AP and therefore OP remineralization were governed by a mechanism other than measured biomass proxies. We identified that APA was strongly associated with F_{fast} relative to POC and BP, thus indicating a potential mechanism for preferential transfer of APA vertically through the water column relative to other biogeochemical parameters (i.e., POC and BP) and for preferential remineralization of P relative to C.

We hypothesize that in this DIP-replete shelf sea environment, the association of APA with fast sinking particles and the resultant influence on vertical distributions of APA in the water column may be linked to enhanced ectoenzyme activity associated with bacteria colonizing particle surfaces and/or release by zooplankton associated with excretion of faecal pellets or during grazing.

This study highlights the potentially significant role of APA in PPhos remineralization in the marine environment. In this N-limited shelf sea environment, APA was not linked with DIP-limitation and was not inhibited at increased DIP concentrations. Surface APA rates in this study were comparable with those of open ocean regions, suggesting that this process may potentially occur in other marine environments. It is essential to better characterize the mechanisms of P cycling and the role of microbes and enzymes in P remineralization in the water column to accurately evaluate nutrient regimes, the efficiency of remineralization and the contribution of regenerated nutrients to primary production in the euphotic layer.

References

Ammerman, J. W. 1993. Microbial cycling of inorganic and organic phosphorus in the water column, p. 621–631. *In* P. F. Kemp, B. F. Sherr, E. B. Sherr, and J. J. Cole (eds.), Handbook of methods in aquatic microbial ecology. Boca Raton, FL: Lewis Publishers.

Anderson, L. A., and J. L. Sarmiento. 1995. Global ocean phosphate and oxygen simulations. Global Biogeochem. Cycles **9**: 621–636. doi:10.1029/95GB01902

Armstrong, F. A. J., P. M. Williams, and J. D. H. Strickland. 1966. Photo-oxidation of organic matter in sea water by ultra-violet radiation, analytical and other applications. Nature **211**: 481–483. doi:10.1038/211481a0

Baltar, F., J. Arístegui, J. M. Gasol, E. Sintes, H. M. van Aken, and G. J. Herndl. 2010. High dissolved extracellular enzymatic activity in the deep central Atlantic Ocean. Aquat. Microb. Ecol. **58**: 287–302. doi:10.3354/ame01377

Barrón, C., and C. M. Duarte. 2015. Dissolved organic carbon pools and export from the coastal ocean. Global Biogeochem. Cycles **29**: 1725–1738. doi:10.1002/2014GB005056

Björkman, K., and D. M. Karl. 1994. Bioavailability of inorganic and organic P compounds to natural assemblages of microorganisms in Hawaiian coastal waters. Mar. Ecol. Prog. Ser. **111**: 265–273. doi:10.3354/meps111265

Boavida, M. J., and R. R. Heath. 1984. Are the phosphatases released by *Daphnia magna* components of its food? Limnol. Oceanogr. **29**: 641–645. doi:10.4319/lo.1984.29.3.0641

Cavan, E. L., F. A. C. Le Moigne, A. J. Poulton, G. A. Tarling, P. Ward, C. J. Daniels, G. M. Fragoso, and R. J. Sanders. 2014. Attenuation of particulate organic carbon flux in the Scotia Sea, Southern Ocean, is controlled by zooplankton fecal pellets. Geophys. Res. Lett. **42**: 821–830. doi:10.1002/2014GL062744

Colman, A. S., R. E. Blake, D. M. Karl, M. L. Fogel, and K. K. Turekian. 2005. Marine phosphate oxygen isotopes and organic matter remineralization in the oceans. Proc. Natl. Acad. Sci. USA. **102**: 13023–13028. doi:10.1073/pnas.0506455102

Conway, D. V. P., and R. Williams. 1986. Seasonal population structure, vertical distribution and migration of the chaetognath *Sagitta elegans* in the Celtic Sea. Mar. Biol. **93**: 377–387. doi:10.1007/BF00401105

Davidson, K., and others. 2007. The influence of the balance of inorganic and organic nitrogen on the trophic dynamics of microbial food webs. Limnol. Oceanogr. **52**: 2147–2163. doi:10.4319/lo.2007.52.5.2147

Davidson, K., L. C. Gilpin, R. Pete, D. Brennan, S. McNeill, G. Moschonas, and J. Sharples. 2013. Phytoplankton and bacterial distribution and productivity on and around Jones Bank in the Celtic Sea. Prog. Oceanogr. **117**: 48–63. doi:10.1016/j.pocean.2013.04.001

Davis, C. E., C. Mahaffey, G. A. Wolff, and J. Sharples. 2014. A storm in a shelf sea: Variation in phosphorus

distribution and organic matter stoichiometry. Geophys. Res. Lett. **41**: 8452–8459. doi:10.1002/2014GL061949

Duhamel, S., S. T. Dyhrman, and D. M. Karl. 2010. Alkaline phosphatase activity and regulation in the North Pacific Subtropical Gyre. Limnol. Oceanogr. **55**: 1414–1425. doi:10.4319/lo.2010.55.3.1414

Duhamel, S., K. M. Björkman, F. Van Wambeke, T. Moutin, and D. M. Karl. 2011. Characterization of alkaline phosphatase activity in the North and South Pacific Subtropical Gyres: Implications for phosphorus cycling. Limnol. Oceanogr. **56**: 1244–1254. doi:10.4319/lo.2011. 56.4.1244

Dyhrman, S. T., and B. P. Palenik. 1999. Phosphate stress in cultures and field populations of the dinoflagellate *Prorocentrum minimum* detected using a single cell alkaline phosphatase activity assay. Appl. Environ. Microbiol. **65**: 3205–3212.

Dyhrman, S. T., and K. C. Ruttenberg. 2006. Presence and regulation of alkaline phosphatase activity in eukaryotic phytoplankton from the coastal ocean: Implications for dissolved organic phosphorus remineralization. Limnol. Oceanogr. **51**: 1381–1390. doi:10.4319/lo.2006.51.3.1381

Gambin, F., G. Bogé, and D. Jamet. 1999. Alkaline phosphatase in a littoral Mediterranean marine ecosystem: Role of the main plankton size classes. Mar. Environ. Res. **47**: 441–456. doi:10.1016/S0141-1136(98)00130-5

Grossart, H. P., K. W. Tang, T. Kiørboe, and H. Ploug. 2007. Comparison of cell-specific activity between free-living and attached bacteria using isolates and natural assemblages. FEMS Microbiol. Lett. **266**: 194–200. doi:10.1111/j.1574-6968.2006.00520.x

Hickman, A. E., P. M. Holligan, C. M. Moore, J. Sharples, V. Krivtsov, and R. M. Palmer. 2009. Distribution and chromatic adaptation of phytoplankton within a shelf sea thermocline. Limnol. Oceanogr. **54**: 525–536. doi:10.4319/lo.2009.54.2.0525

Hickman, A. E., C. Moore, J. Sharples, M. I. Lucas, G. H. Tilstone, V. Krivtsov, and P. M. Holligan. 2012. Primary production and nitrate uptake within the seasonal thermocline of a stratified shelf sea. Mar. Ecol. Prog. Ser. **463**: 39–57. doi:10.3354/meps09836

Hoppe, H.-G., S. J. Kim, and K. Gocke. 1988. Microbial decomposition in aquatic environments: Combined process of extracellular enzyme activity and substrate uptake. Appl. Environ. Microbiol. **54**: 784–790.

Hoppe, H.-G., and S. Ullrich. 1999. Profiles of ectoenzymes in the Indian Ocean: Phenomena of phosphatase activity in the mesopelagic zone. Aquat. Microb. Ecol. **19**: 139–148. doi:10.3354/ame019139

Jamet, D., and G. Boge. 1998. Characterisation of marine zooplankton alkaline phosphatase activity in relation to water quality. Hydrobiologia **373**: 311–316. doi:10.1023/A:1017008430088

Jansson, M. 1976. Phosphatases in lake water characterization of enzymes from phytoplankton and zooplankton by gel filtration. Science **194**: 320–321. doi:10.1126/science.184531

Karl, D. M., J. E. Dore, D. V. Hebel, and C. Winn. 1991. Procedures for particulate carbon, nitrogen, phosphorus and total mass analyses used in the US-JGOFS Hawaii Ocean time-series program, p. 71–77. *In* D. C. Hurd and D. Spencer (eds.) Marine particles: Analysis and characterization.

Karl, D. M., and G. Tien. 1992. MAGIC: A sensitive and precise method for measuring dissolved phosphorus in aquatic environments. Limnol. Oceanogr. **37**: 105–116. doi:10.4319/lo.1992.37.1.0105

Karl, D. M., and K. M. Björkman. 2002. Dynamics of DOP, p. 249–366. *In* D. A. Hansell and C. A. Carlson [eds.], Biogeochemistry of marine dissolved organic matter. Elsevier Science.

Karner, M., and G. J. Herndl. 1992. Extracellular enzymatic activity and secondary production in free-living and marine-snow-associated bacteria. Mar. Biol. **113**: 341–347. doi:10.1007/BF00347289

Kirchman, D. 1993. Particulate detritus and bacteria in marine environments, p. 321–341. *In* T. F. Ford [ed.], Aquatic microbiology: An ecological approach. Blackwell Scientific.

Kirchman, D. 2001. Measuring bacterial biomass production and growth rates from leucine incorporation in natural aquatic environments. Methods Microbiol. **30**: 227–237. doi:10.1016/S0580-9517(01)30047-8

Koike, I., and T. Nagata. 1997. High potential activity of extracellular alkaline phosphatase in deep waters of the central Pacific. Deep-Sea Res. Part II Top. Stud. Oceanogr. **44**: 2283–2294. doi:10.1016/S0967-0645(97)00025-8

Kolowith, L. C., E. D. Ingall, and R. Benner. 2001. Composition and cycling of marine organic phosphorus. Limnol. Oceanogr. **46**: 309–320. doi:10.4319/lo.2001.46.2.0309

Labry, C., D. Delmas, A. Youenou, J. Quere, A. Leynaert, S. Fraisse, M. Raimonet, and O. Rageuneau. 2016. High alkaline phosphatase activity in phosphate replete waters: The case of two macrotidal estuaries. Limnol. Oceangr. **61**: 1513–1529. doi:10.1002/lno.10315

Li, H., M. J. W. Veldhuis, and A. F. Post. 1998. Alkaline phosphatase activities among planktonic communities in the northern Red Sea. Mar. Ecol. Prog. Ser. **173**: 107–115. doi:10.3354/meps173107

Lomas, M. W., A. L. Burke, D. A. Lomas, D. W. Bell, C. Shen, S. T. Dyhrman, and J. W. Ammerman. 2010. Sargasso Sea phosphorus biogeochemistry: An important role for dissolved organic phosphorus (DOP). Biogeosciences **7**: 695–710. doi:10.5194/bg-7-695-2010

Luo, H., R. Benner, R. A. Long, and J. Hu. 2009. Subcellular localization of marine bacterial alkaline phosphatases. Proc. Natl. Acad. Sci. USA. **106**: 21219–21223. doi:10.1073/pnas.0907586106

Mahaffey, C., S. Reynolds, C. E. Davis, and M. C. Lohan. 2014. Alkaline phosphatase activity in the subtropical

ocean: Insights from nutrient, dust and trace metal addition experiments. Front. Mar. Sci. **1**: 1–13. doi:10.3389/fmars.2014.00073

Mather, R. L., and others. 2008. Phosphorus cycling in the North and South Atlantic Ocean subtropical gyres. Nat. Geosci. **1**: 439–443. doi:10.1038/ngeo232

McCarthy, S. D. S., S. P. Rafferty, and P. C. Frost. 2010. Responses of alkaline phosphatase activity to phosphorus stress in *Daphnia magna*. J. Exp. Biol. **213**: 256–261. doi:10.1242/jeb.037788

Monbet, P., I. D. McKelvie, A. Saefumillah, and P. J. Worsfold. 2007. A protocol to assess the enzymatic release of dissolved organic phosphorus species in waters under environmentally relevant conditions. Environ. Sci. Technol. **41**: 7479–7485. doi:10.1021/es070573c

Moore, C. M., D. J. Suggett, A. E. Hickman, Y.-N. Kim, J. F. Tweddle, J. Sharples, R. Geider, and P. M. Holligan. 2006. Phytoplankton photoacclimation and photoadaptation in response to environmental gradients in a shelf sea. Limnol. Oceanogr. **51**: 936–949. doi:10.4319/lo.2006.51.2.0936

Murphy, J., and J. P. Riley. 1962. A modified single solution method for the determination of phosphate in natural waters. Anal. Chim. Acta **27**: 31–36. doi:10.1016/S0003-2670(00)88444-5

Nicholson, D., S. Dyhrman, F. Chavez, and A. Paytan. 2006. Alkaline phosphatase activity in the phytoplankton communities of Monterey Bay and San Francisco Bay. Limnol. Oceanogr. **51**: 874–883. doi:10.4319/lo.2006.51.2.0874

Orchard, E. D., E. A. Webb, and S. T. Dyhrman. 2009. Molecular analysis of the phosphorus starvation response in Trichodesmium spp. Env. Microbiol. **11**: 2400–2411. doi:10.1111/j.1462-2920.2009.01968.x

Orchard, E. D., J. W. Ammerman, M. W. Lomas, and S. T. Dyhrman. 2010. Dissolved inorganic and organic phosphorus uptake in *Trichodesmium* and the microbial community: The importance of phosphorus ester in the Sargasso Sea. Limnol. Oceanogr. **55**: 1390–1399. doi:10.4319/lo.2010.55.3.1390

Pemberton, K., A. P. Rees, P. I. Miller, R. Raine, and I. Joint. 2004. The influence of water body characteristics on phytoplankton diversity and production in the Celtic Sea. Cont. Shelf Res. **24**: 2011–2028. doi:10.1016/j.csr.2004.07.003

Rees, A. P., S. B. Hope, C. E. Widdicombe, J. L. Dixon, E. M. S. Woodward, and M. F. Fitzsimons. 2009. Alkaline phosphatase activity in the western English Channel: Elevations induced by high summertime rainfall. Estuar. Coast. Shelf Sci. **81**: 569–574. doi:10.1016/j.ecss.2008.12.005

Rengefors, K., K. C. Ruttenberg, C. Haupert, C. Taylor, B. L. Howes, and D. M. Anderson. 2003. Experimental investigation of taxon-specific response of alkaline phosphatase activity in natural freshwater phytoplankton. Limnol. Oceanogr. **48**: 1167–1175. doi:10.4319/lo.2003.48.3.1167

Reynolds, S., C. Mahaffey, V. Roussenov, and R. G. Williams. 2014. Evidence for production and lateral transport of dissolved organic phosphorus in the eastern subtropical North Atlantic. Global Biogeochem. Cycles **28**: 805–824. doi:10.1002/2013GB004801

Riley, J. S., R. Sanders, C. Marsay, F. A. C. Le Moigne, E. P. Achterberg, and A. J. Poulton. 2012. The relative contribution of fast and slow sinking particles to ocean carbon export. Global Biogeochem. Cycles **26**: 1–10. doi:10.1029/2011GB004085

Sebastián, M., J. Arístegui, M. F. Montero, and F. X. Niell. 2004. Kinetics of alkaline phosphatase activity, and effect of phosphate enrichment: A case study in the NW African upwelling region. Mar. Ecol. Prog. Ser. **270**: 1–13. doi:10.3354/meps270001

Sebastian, M., and J. W. Ammerman. 2009. The alkaline phosphatase PhoX is more widely distributed in marine bacteria than the classical PhoA. ISME J. **3**: 563–572. doi:10.1038/ismej.2009.10

Sharples, J., and others. 2007. Spring-neap modulation of internal tide mixing and vertical nitrate fluxes at a shelf edge in summer. Limnol. Oceanogr. **52**: 1735–1747. doi:10.4319/lo.2007.52.5.1735

Sharples, J., C. M. Moore, A. E. Hickman, P. M. Holligan, J. F. Tweddle, M. R. Palmer, and J. H. Simpson. 2009. Internal tidal mixing as a control on continental margin ecosystems. Geophys. Res. Lett. **36**: L23603. doi:10.1029/2009GL040683

Smith, D. C., M. Simon, A. L. Alldredge, and F. Azam. 1992. Intense hydrolytic enzyme activity on marine aggregates and implications for rapid particle dissolution. Nature **359**: 139–142. doi:10.1038/359139a0

Sohm, J. A., and D. G. Capone. 2006. Phosphorus dynamics of the tropical and subtropical North Atlantic: Tichodesmium spp. versus bulk plankton. Mar. Ecol. Prog. Ser. **317**: 21–28. doi:10.3354/meps317021

Sohm, J. A., C. Mahaffey, and D. G. Capone. 2008. Assessment of relative phosphorus limitation of Trichodesmium spp. in the North Pacific and Atlantic and the north coast of Australia. Limnol. Oceanogr. **53**: 2495–2502. doi:10.4319/lo.2008.53.6.2495

Suzumura, M., F. Hashihama, N. Yamada, and S. Kinouchi. 2012. Dissolved phosphorus pools and alkaline phosphatase activity in the euphotic zone of the Western North Pacific Ocean. Front. Microbiol. **3**: 99. doi:10.3389/fmicb.2012.00099

Tamburini, C., M. Garel, B. Al Ali, B. Mérigot, P. Kriwy, B. Charrière, and G. Budillon. 2009. Distribution and activity of Bacteria and Archaea in the different water masses of the Tyrrhenian Sea. Deep-Sea Res. Part II Top. Stud. Oceanogr. **56**: 700–712. doi:10.1016/j.dsr2.2008.07.021

Tang, K. W., R. N. Glud, A. Glud, S. Rysgaard, and T. G. Neilsen. 2011. Copepod guts as biogeochemical hotspots in the sea: Evidence from microelectrode profiling of *Calanus* spp. Limnol. Oceanogr. **56**: 666–672. doi:10.4319/lo.2011.56.2.0666

Tweddle, J. F., J. Sharples, M. R. Palmer, K. Davidson, and S. McNeill. 2013. Enhanced nutrient fluxes at the shelf sea seasonal thermocline caused by stratified flow over a bank. Prog. Oceanogr. **117**: 37–47. doi:10.1016/j.pocean.2013. 06.018

Tyrrell, T. 1999. The relative influences of nitrogen and phosphorus on oceanic primary production. Nature **400**: 525–531. doi:10.1038/22941

Vidal, M., C. M. Duarte, S. Agustí, J. M. Gasol, and D. Vaqué. 2003. Alkaline phosphatase activities in the central Atlantic Ocean indicate large areas with phosphorus deficiency. Marine Ecology Progress Series **262**: 43–53. doi:10.3354/meps262043

Williams, C. A., J. Sharples, C. Mahaffey, and T. Rippeth. 2013. Wind-driven nutrient pulses to the subsurface chlorophyll maximum in seasonally stratified shelf seas. Geophys. Res. Lett. **40**: 5467–5472. doi:10.1002/2013GL058171

Williams, R. 1985. Vertical distribution of *Calanus finmarchicus* and *C. helgolandicus* in relation to the development of the seasonal thermocline in the Celtic Sea. Mar. Biol. **86**: 145–149. doi:10.1007/BF00399020

Yamamuro, M., and H. Kayanne. 1995. Rapid direct determination of organic carbon and nitrogen in carbonate-bearing sediments with a Yanaco MT-5 CHN analyzer. Limnol. Oceanogr. **40**: 1001–1005. doi:10.4319/lo.1995.40.5.1001

Acknowledgments

We thank colleagues and crew on RRS James Cook (cruise JC025), RRS Discovery (D352 and DY026) and the British Oceanographic Data Centre for providing calibrated CTD data. We thank E. Cavan for help with marine snow catcher deployments and helpful discussions that aided analysis and data interpretation. We thank Sharon McNeil and Keith Davidson of the Scottish Marine Association for providing bacterial abundance and bacterial production data. We would like to thank the reviewers for their constructive comments and the Editor for support and guidance throughout this process. Data, protocols, methods, and derived data products are available from the corresponding author upon request. This work was supported by the UK Natural Environment Research Council's (NERC) Oceans2025 Programme and joint NERC-DEFRA support through Grant NE/F001983/1 (JC025) awarded to J. Sharples, joint NERC-DEFRA support through the Shelf Sea Biogeochemistry Programme Grant NE/K002007/1 (DY026) awarded to J. Sharples, C. Mahaffey, and G. Wolff, and support for NERC Responsive Mode Research Project Grant NE/F002432/1 (D352) awarded to T. Rippeth and J. Sharples.

Conflict of Interest

None declared.

Submitted 26 February 2016
Revised 28 July 2016; 18 January 2017
Accepted 22 February 2017

Associate editor: Josette Garnier